Infrared Multiphoton Excitation of Small Molecules

N. BLOEMBERGEN, I. BURAK,* E. MAZUR AND T. B. SIMPSON**
Gordon McKay Laboratory, Division of Applied Sciences,
Harvard University, Cambridge, MA 02138 USA

(*Received 31 December 1983*)

Abstract. The collisionless infrared multiphoton excitation of small molecules, OCS, SO_2, NO_2 and DN_3 is discussed. Despite the small absorbance of IR photons by these molecules, evidence for the population of highly excited vibronic levels below the dissociation threshold is obtained. Multiphoton dissociation is observed, as well. The average number of photons absorbed and dissociation yields depend predominately on the laser intensity. High order multiphoton processes couple the ground vibrational level with the quasicontinuum of excited levels below and above the dissociation threshold.

I. INTRODUCTION

Since the first demonstration of collisionless multiphoton excitation in SF_6,[1] an intensive study of this phenomenon has been carried out. Today more than a hundred molecular systems are reported to undergo infrared multiphoton excitation or dissociation (IRMPE or IRMPD) under the action of high fluence CO_2 laser pulses.[2] The IRMPE of moderate and large sized molecules ($N \geqq 6$) is fairly well understood.[3] The molecular vibrational manifold is divided into three energy regions. In the lowest energy region (Region I) the density of molecular levels is very low, and the laser field interacts coherently with isolated molecular levels.

As the vibrational energy increases, the density of vibrational states grows. Due to anharmonic terms in the vibrational Hamiltonian, the normal mode oscillator strength is spread over many levels contained in a frequency interval Γ. At a certain level of vibrational energy the field-molecular coherence is destroyed and the dynamics of the excitation is described by a set of rate equations:

$$\frac{dP_n}{dt} = -[(\sigma_{n,n-1} + \sigma_{n,n+1})P_n - \sigma_{n-1,n}P_{n-1} - \sigma_{n+1,n}P_{n+1}]I, \quad (1)$$

where P_n is the occupation probability of the nth energy shell and $\sigma_{n,n+1}$ is the one-photon cross section for the $n \rightarrow n \pm 1$ transition and I the phton flux. This energy region is referred to as Region II or the quasicontinuum. From integration of Eq. (1) it follows that P_n depends on the laser fluence only. It has been demonstrated experimentally that the IRMPE of SF_6 is indeed mainly determined by the laser fluence.[4]

When a molecule is pumped by an intense IR laser pulse, the ground state may be directly coupled to Region II by a coherent multiphoton process or through a multistep absorption process involving population of intermediate Region I levels. In the latter case the energies of the intermediate levels i should exactly fulfill the resonance condition, $E_i - E_g = nh\nu_L$.

For a given molecular system the onset of Region II is determined by several parameters: the density of vibrational levels $\rho(E)$, the Rabi frequency $\hbar^{-1}|\mu\mathscr{E}|$, the spread in the oscillator strength Γ and the laser frequency width $\Delta\omega_L$. For a transform-limited pulse of duration t_p, one has $\Delta\omega_L = (2\pi t_p)^{-1}$. For the weak coupling case defined by $\hbar^{-1}|\mu\mathscr{E}| < \Delta\omega_L < \Gamma$, the quasicontinuum is established at a vibrational energy level where

$$\rho^{-1}(E) < \Delta\omega_L. \quad (2)$$

For the dipole moment appearing in the Rabi frequency term, one can take either the IR active normal mode dipole strength or an effective dipole obtained by averaging the transition dipole between the true nuclear molecular eigenstates (NME)[5,6] over a range Γ. A different characterization of the quasicontinuum for intermediate or strong coupling cases is given elsewhere.[7]

The third energy region denoted by Region III lies above the dissociation threshold. The energy levels in this region are characterized by a dissociative width, and an additional term, $-k^n_{diss}P_n$, has to be added to the rate equation (1), with k^n_{diss} the unimolecular dissociation rate at energy E_n.

In contrast with the case for larger molecules, the IRMPE of small molecules is less well understood both theoretically and experimentally. For diatomics IRMPE has not been observed experimentally. Theoretical calculation for HF[8] indicate that intensities of 10^{13} W/cm^2 would be required to dissociate the molecule. At these high fields ionization and electric breakdown cannot be avoided. The vibrational densities of triatomic and four-atom molecules are higher than in the diatomic case. They are still too low, however, to satisfy quasicontinuum conditions. The densities of the vibrational states for some of the molecules studied in this work are plotted in Fig. 1. It is seen that even close to the dissociation threshold the densities are below 100 states per wave number.

When small molecules are exposed to a strong IR field, intermediate states can be populated provided n photon resonances are met. However, direct coupling to the dissociative continuum should also be considered. In such a case near resonances of intermediate levels play a

* *Permanent address*: Department of Chemistry, Tel Aviv University, Tel Aviv, Israel.
** *Current address*: Harry Diamond Laboratories, 2800 Powder Mill Road, Adelphi, MD 20783 USA.

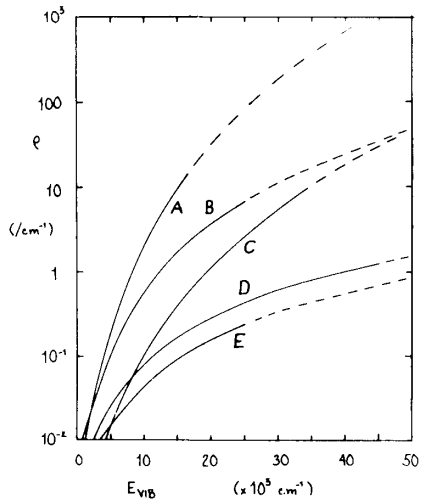

Fig. 1. Whitten–Rabinovitch calculation of the vibrational density, as a function of vibrational energy. The curves correspond to the following molecules: (A) DN_3; (B) OCS; (C) NH_3; (D) SO_2; (E) NO_2.

crucial role in determining the efficiency of the MPD process. It should be emphasized that the near-resonant intermediate levels have no final population. Although the diagonal matrix elements of intermediate levels may increase temporarily due to power broadening, they adiabatically follow the laser pulse.[9]

IRMPD of SO_2,[10] OCS,[11] NH_3[12] and HN_3[13] with long ($t_p > 100$ ns) CO_2 laser pulses has been reported. However, the excitation of SO_2 and NH_3 has been carried out at high pressures ($p > 1$ torr), so that the collisionless character of the excitation may be questioned. Furthermore, for HN_3 no analysis has been carried out to exclude the role of collisions during the IR excitation. For OCS conflicting results have been obtained. A dissociation yield of unity has been reported in a molecular beam experiment,[11] while no significant dissociation has been observed by us for OCS in cells at low pressure.

The main objectives of this work are the establishment and characterization of the collisionless MPE and MPD process in OCS, SO_2, NO_2, and DN_3. The IRMPD of NH_3 will be reported elsewhere.

The results show that there is a gradual transition in the MPE and MPD characteristics from diatomic to large molecules.

II. EXPERIMENTAL

The experimental apparatus has been described in detail previously.[4,14] A tunable CO_2 laser capable of generating pulses of variable duration is used. IRMPE pumping has been carried out using pulses of 0.1, 0.5, 30, and 100 ns duration. The CO_2 laser is focused into a cell. The degree of focusing depends upon the desired fluences or peak intensities. Fluences up to 300 J cm^{-2} and peak intensities of 500 GW are required to detect MPD in small molecules.

Diagnostics of the MPE or MPD process have been carried out using the following methods:

(a) Visible and UV emission induced by the IR pulse has been measured.

(b) A microphone has been used to detect IR photoacoustic signals.

(c) Introduction of scavenger molecules into the absorption cell has been used to detect specific atomic dissociation products.

All signals are collected and stored in a home-built DEC LSI-11 based data acquisition system. Transient signals are digitized by a Biomation 8100 wave form recorder.

III. IRMPE OF OCS

Optoacoustic methods detect a measurable absorption in the OCS at the P(24) line of the 9.4 μm branch of the CO_2 laser.[15] Yet the infrared absorption of OCS is too small for absolute calibration into $\langle n \rangle$, the average number of photons absorbed per molecule. Instead, the calibration is achieved in the following way. Mixtures of 5 torr OCS and 0.1 torr of SF_6 are irradiated with 0.5 ns CO_2 laser pulses. The system is first irradiated at the P(20) 10.6 μm branch where SF_6 absorbs. The optoacoustic signals are calibrated to energy absorbed, using known $\langle n \rangle$ values for SF_6.[4] The CO_2 laser is then tuned to the P(24) 9.4 μm branch transition where SF_6 does not absorb, and the optoacoustic signals are measured. The $\langle n \rangle$ photon absorbance for OCS is shown in Fig. 2 as a function of the intensity or fluence of the IR pulses of 0.5 ns duration. It is shown that the average number of photons absorbed per molecule is less than unity, up to fluences of 200 J cm^{-2} and intensities of 300 GW cm^{-2}. This measurement contradicts an earlier report[11] by others, who claimed a complete dissociation at fluences of 60 J cm^{-2} and intensities of only 0.2 GW cm^{-2}, although no dissociation products were detected. Their claim was based on a disappearance of the molecular beam from a straight-throughput detector. A deflection of the exposed molecular beam induced by the inhomogeneous electric field of the crossed CO_2 laser beam has been suggested to account for the discrepancy between the two experiments.[15] The small number of photons absorbed by OCS does not imply the absence of high excitation or dissociation. Only a small fraction of the ground state population may interact with the CO_2 radiation. Moreover, the MPD yield for this particular rotational level may be exceedingly small. An attempt has been made to detect sulphur and oxygen atomic dissociation products. Nitric oxide has been mixed with OCS. If dissociation into CS and O occurs, the oxygen atoms should be scavenged by NO to produce fluorescing NO_2 in a three-body recombination process. No such emission has been observed. However, positive evidence for the MPD of OCS into CO + S has been obtained. When NO_2 is admixed with OCS, an increase of the

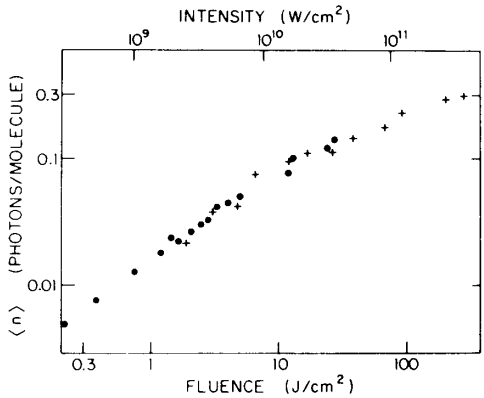

Fig. 2. Log-log plot of the average number of photons absorbed per OCS molecule $\langle n \rangle$, as a function of the fluence or intensity of the CO_2 laser pulse. The laser is tuned to P(24), 9.4 μm branch. Laser pulse width is 0.5 ns.

optoacoustic signal is observed.[7] This is attributed to the following rapid exothermic reactions[16]:

$$S + NO_2 \rightarrow SO + NO + 2\ eV, \quad (3a)$$

$$SO + NO_2 \rightarrow SO_2 + NO + 2.5\ eV. \quad (3b)$$

The dissociation yields have been estimated from calculation of the additional energy detected by the microphone when NO_2 is added, taking into account the thermochemical data. For 0.5 ns CO_2 pulses of 200 J cm^{-2}, a value of $(6 \pm 4) \times 10^{-4}$ is obtained. The pressures of OCS and NO_2 in the measured sample are 5 torr and 0.5 torr, respectively. The MPE and MPD processes for OCS show a strong dependence on intensity. Longer pulses with the same total fluence give unobservably small signals. Unfortunately, due to the small signal and consequently the large scatter of the data, the pressure dependence of the signals could not be measured. The MPE process could have been assisted by the rare collisions that occur during the short period of excitation. A claim for the collisionless MPE process in the bulk must be confirmed by appropriate scaling with the pressure. This has been carried out successfully for the IRMPE data of other molecules, as described in the next sections.

IV. IRMPE OF SO_2

The ν_1 stretch mode of SO_2 is centered at 1150 cm^{-1} and the anharmonicity is 5 cm^{-1}. This is 70 cm^{-1} higher than the center of the R branch of the 9.4 μm CO_2 laser transition. Despite the energy mismatch, measurable photoacoustic signals are recorded for SO_2 when irradiated with intense 0.5 ns CO_2 laser pulses.[17] The calibrated absorbance of SO_2 as a function of the fluence of the 0.5 ns laser pulse is shown in Fig. 3. Irradiation of SO_2 with longer 30 ns pulses resulted in negligible optoacoustic signals. The average number of photons absorbed by the 0.5 ns pulse is far below unity. Still, the observation of UV emission from the irradiated sample is evidence for multiphoton excitation to highly excited vibrational states. Due to the breakdown of the Born–Oppenheimer approximation,[18] the highly excited vibrational levels of SO_2 are slightly admixed with vibronic levels of excited electronic states. As a result, the vibronic manifold between 25,000 cm^{-1} and the dissociation threshold is characterized by a broad band fluorescence[19] with radiative lifetimes of 20 μs–200 μs.[20,21] The induced fluorescence signal extending from 300 nm to 500 nm, in agreement with the SO_2 fluorescence spectrum, is shown in Fig. 4. The observed rise time of two points corresponds to the instrumental time resolution. The decay time of the fluorescence scales inversely with pressure, while the amplitudes exhibit a linear dependence on the pressure, thus confirming the collisionless character of the MPE process.

The fraction of molecules excited to the radiative region, Y_{exc}, is plotted as a function of intensity of 0.5 ns pulses in Fig. 5. Calibration of the fluorescence amplitudes with the excitation yields, Y_{exc}, is achieved as follows. The initial rate of photon emission from the excitation region is estimated from the photomultiplier signal gain and wavelength characteristics and the solid angle viewed by the photomultiplier. The rate of photon

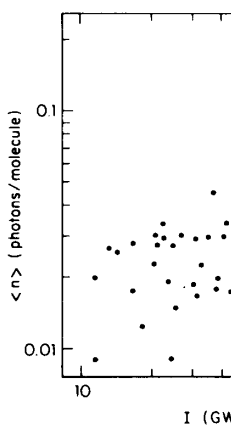

Fig. 3. Log-log plot of the average number of photons absorbed per SO_2 molecule as a function of CO_2 laser intensity. Laser is tuned to R(22) 9.4 μm CO_2 transition.

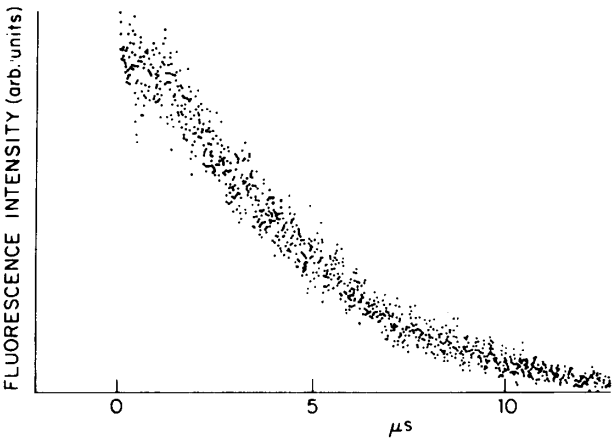

Fig. 4. Transient fluorescence signal from a 90 mtorr SO_2 sample induced by 0.5 ns CO_2 laser pulses. Points are digitized averages of 50 laser pulses.

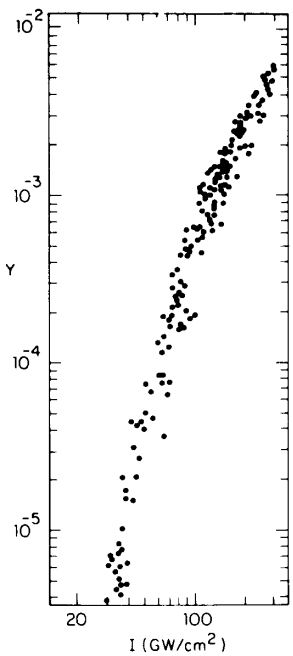

Fig. 5. Log-log plot of the yield of SO_2 molecules excited to the fluorescent region, as a function of the CO_2 laser intensity.

emission is proportional to N_{exc}, the number of excited SO_2 molecules and the average inverse radiative lifetime τ_{rad}^{-1} of SO_2. A value of 100 μs has been taken for τ_{rad}, the average radiative lifetime of SO_2. The value Y_{exc} is finally obtained from the ratio N_{exc}/N_0, where N_0 is the number of SO_2 molecules in the focused region. The volume V_{eff} of the latter is given by

$$V_{eff} = \pi w_0^2 Z_0/2, \tag{4}$$

where w_0 is the beam waist and Z_0 is the confocal beam parameter. No emission is observed when the system is irradiated with CO_2 pulses of 30 ns duration or longer.

Multiphoton dissociation induced by high intensity CO_2 pulses is also detected. When adding nitric oxide as a scavenger to the system, the atomic oxygen dissociation product reacts with NO in a three-body collision process to form excited NO_2^* in the reaction

$$O + 2NO \xrightarrow{k_0} NO_2^* + NO.$$

NO_2^* is a molecule formed in a highly excited vibronic level of the ground electronic state. Those states are slightly admixed with vibronic states of excited electronic levels. They therefore possess oscillator strength for optical emission in the visible. Since the emission of NO_2^* is shifted further to the red than the SO_2^* fluorescence, the emissions from the two species are well separated.

The time evolution of the excited NO_2^* molecules is described by the following rate equations:

$$\frac{d[O]}{dt} = -k_0[O][NO]^2, \tag{5}$$

$$\frac{d[NO_2^*]}{dt} = -k_{rad}^{NO_2}[NO_2^*] - k_1[NO][NO_2] + k_0[O][NO]^2, \tag{6}$$

where $k_{rad}^{NO_2}$ is the average radiative lifetime of excited NO_2 and k_1 is the collisional quenching rate. Since the chemiluminescence of NO_2^* has been studied in mixtures involving a high $[NO]/[SO_2]$ ratio, three-body recombination terms involving SO_2 have been neglected in Eq. (6). For the same reason, collisional quenching of NO_2^* with SO_2 has also been disregarded. Integration of Eqs. (5) and (6) yields

$$[O] = [O]_0 \exp(-k_0[NO]^2 t). \tag{7}$$

Since $k_0 \ll k_1,\ k_{rad}^{NO_2}$,

$$[NO_2^*] = \frac{k_0}{k_1}[NO][O]_0 \exp(-k_0[NO]^2 t). \tag{8}$$

Here $[O]_0$ is the initial concentration of oxygen atoms following the short 0.5 ns laser pulse. The decay time of the excited NO_2^* is found to be inversely proportional to the square of the [NO] density, with a rate constant k_0 of 200 s^{-1} $torr^{-2}$. The number of dissociated SO_2 molecules N_{diss} is found to be

$$N_{diss} = [O]_0 V_{eff},$$

where V_{eff} is defined in Eq. (4). This number may be estimated from the initial amplitude of the chemiluminescence signal I_{chem},

$$I_{chem} = k_{rad}^{NO_2} \frac{k_0}{k_1} N_{diss}[NO]. \tag{9}$$

The value of N_{diss} has been obtained by estimating the photon emission rates and the use of Eq. (8). A value of 50 μs has been used for the average radiative lifetime of NO_2.[22] A value of 2×10^6 s^{-1} $torr^{-1}$ has been used for k_1.[22] The absolute dissociation yield Y_{diss} is obtained by dividing N by the number of SO_2 molecules in the focused volume. Values of Y_{diss} vs. the CO_2 intensity are shown in Fig. 6. It is interesting to compare values of $\langle n \rangle$, Y_{exc} and Y_{diss} for the same fluence or peak intensity. When the ground state is directly coupled to the dissociative region, the number of photons absorbed per molecule $\langle n \rangle$ should be $42 \times Y_{diss}$ photons, since 42 photons are required to reach the dissociation threshold. For a direct coupling between the ground state and fluorescent levels, $\langle n \rangle$ should be about $n' Y_{diss}$ with $25 < n' < 42$. In fact, $\langle n \rangle$ is found to be 100 times greater than the sum $Y_{diss} + Y_{exc}$. This suggests a direct MP coupling of the ground state levels of SO_2 with the denser fluorescent region or the dissociative region. Moreover, by comparing Figs. 5 and 6, Y_{diss} grows somewhat more rapidly than Y_{exc}. It appears that once excitation to the fluorescent region is achieved, further excitation to the dissociative region is relatively more efficient.

Preparation of vibrationally excited SO_2 in the fluorescent region is possible through the absorption of one UV photon. Indeed, it has been established[23] that SO_2 molecules thus excited do interact with low fluence, long ($t_p \sim 100$ ns) CO_2 pulses. These experiments suggest that the fluorescent region may act as the quasicontinuum Region II for this triatomic molecule. Similar experiments have been carried out on NO_2,[24] and an extended diagnosis of the IRMPE of optically prepared NO_2 molecules has been published.[14] These experiments are briefly reviewed in the next section.

V. IRMPE OF OPTICALLY PREPARED NO_2 MOLECULES

Since the infrared active modes of NO_2 are too far removed from CO_2 laser frequencies, no observable excitation occurs for infrared excitation from the ground state even at intensities of 300 GW cm^{-2}. As in SO_2, the highly excited vibrational manifold of the electronic ground state is slightly admixed with excited electronic states. As a result, on absorbing a visible photon, the molecule is prepared in an excited state which has the

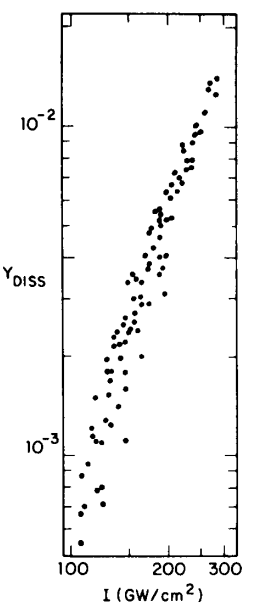

Fig. 6. Dissociation yield of SO_2 vs. CO_2 laser intensity.

dominant character of a highly excited vibronic level of the electronic ground state. In our experiments NO_2 is first pumped with a visible dye laser. An IR excitation with a CO_2 laser then follows, and changes in the visible fluorescence are observed. The IRMPE of the prepared NO_2 is studied as a function of the optical excitation energy in the following way. The vibrational energy manifold of NO_2 is divided into subregions (see Fig. 7). Subregion 1 consists of a vibrational level confined between the dissociation threshold E_{diss} at 25,137 cm^{-1} and $E - h\nu_{CO_2}$ where $h\nu_{CO_2}$ is the CO_2 laser photon energy. Subregion 2 is limited by $E_{diss} - h\nu_{CO_2}$ and $E_{diss} - 2h\nu_{CO_2}$, etc.

When excited with a pulse of wavelength λ_{exc}, the excited NO_2 molecule fluoresces with a broad-band spectrum extending from λ_{exc} far into the red. In the absence of CO_2 radiation no anti-Stokes emission is observed on the blue side. When the fluorescence is observed with a narrow-band filter with λ_{obs} close to λ_{exc}, the observed fluorescence monitors the emission from the particular energy levels prepared by the dye laser pulse. It has been established[24] that the fluorescence monitored by a long pass filter with a cut at 600 nm is insensitive to the specific distribution over different subregions. The broad-band fluorescence thus monitors the total population of the excited NO_2, as long as the vibrational excitation remains above an energy corresponding to the cutoff frequency.

Figure 8a shows the changes in the fluorescence signals when NO_2, initially prepared in subregion 1, is exposed to 0.5 ns CO_2 pulses. At low CO_2 fluences two main processes take place: upward excitation to the dissociative region and downward transition to subregion 2. The decrease of the broad band red signal with increasing CO_2 fluence is proportional to dissociation yield of the initially excited NO_2 molecules. In contrast, the drop of the narrow-band fluorescence is due to upward dissociative pumping as well as to a downward transition from subregion 1 to subregion 2. This explains why the upper curve in Fig. 8a drops more slowly with CO_2 energy than the lower curve does. Moreover, the initial slopes of the upper and lower curves are proportional to the cross sections σ_{10} and $\sigma_{10} + \sigma_{12}$, respectively. Here σ_{10} and σ_{12} are the cross sections for upward and downward pumping from subregion 1, respectively. Figure 8b shows the induced changes in the fluorescence signals when the system is initially prepared in subregion 2. The upper curve monitors the total population of excited NO_2 molecules while the lower monitors the subregion 1 population. As the fluence is increased, further pumping of the subregion 1 molecule leads to dissociation and subsequent drop in the narrow-band anti-Stokes fluorescence.

Excitations to subregion 3 have also been carried out and are described elsewhere.[14] One should point out that the fluences needed to dissociate the NO_2 via two-photon transitions are about 1 J cm^{-2}. A fluence of 5 J cm^{-2} is required to dissociate a significant portion of NO_2 initially prepared in subregion 3. Those fluences should be compared with the 300 J cm^{-2} fluence required to observe a small yield dissociation for other triatomic molecules in the ground vibrational level.

Fluorescence curves corresponding to the preparation of NO_2 in subregions 1, 2, 3, and IR excitation with 0.5 ns CO_2 pulses have been fitted with a rate equation model (see Eq. (1)). The cross sections $\sigma_{10}, \sigma_{12}, \ldots, \sigma_{65}$ have been determined. These cross sections remain the same for 0.1 ns pulses. In contrast, a considerable change in IRMPE dynamics is observed for longer 30 ns pulses. The efficiency of the long pulses in promoting transitions within the bound manifold of NO_2 is decreased by about an order of magnitude when compared with short pulses of the same fluence. Not unexpectedly the σ_{10} cross sections for the upward pumping into the dissociative region are independent of the pulse length. The dissociative region is a true continuum and Fermi's Golden Rule should be obeyed.

It appears that the requirement for a quasicontinuum (2) is satisfied for the short pulses only. This sets a lower limit for the required density of states $\rho \sim 10$ per cm^{-1}. However, even at the dissociation threshold, the vibrational density of NO_2 is still too low (see Fig. 1) to satisfy condition (2). A strong rotational-vibrational coupling has been observed[14,25] for highly excited vibrational levels of NO_2. This suggests that vibrational-rotational section rules break down and the quasicontinuum consists of the

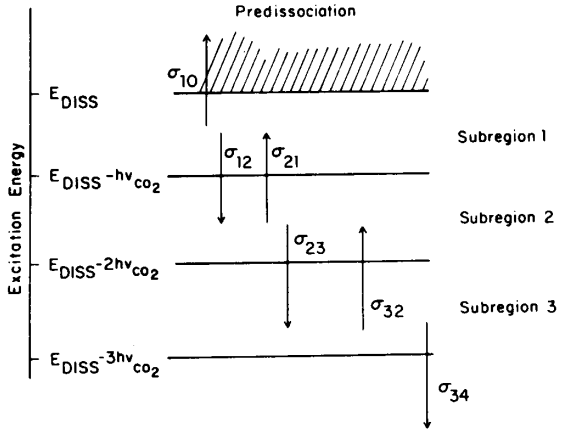

Fig. 7. Schematic diagram showing division of the vibrational energy manifold into energy subregions.

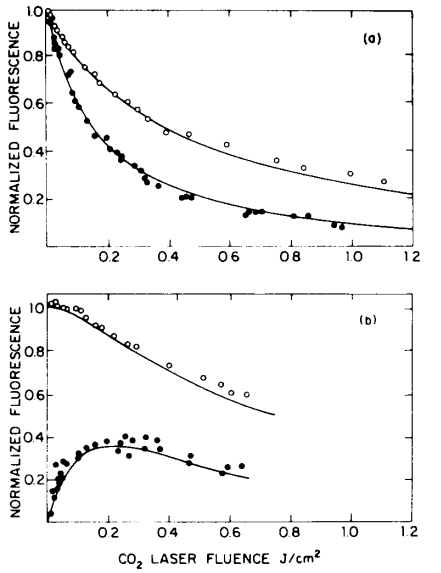

Fig. 8. NO_2 fluorescence yields as a function of the fluence of 0.5 ns CO_2 laser pulse. ○ red fluorescence, ● narrow band fluorescence. (a) NO_2 is first prepared in subregion 1. (b) NO_2 is first prepared in subregion 2.

denser vibrational-rotational manifold. Indeed, if NO_2 is initially cooled by supersonic expansion to very low rotational J values and then optically excited, no IRMPE is observed.[26]

VI. IRMPE OF DN_3

The P(18) line of the 10.6 μm CO_2 laser at 946 cm^{-1} is resonant with the ν_4 mode of this molecule. If more than 18 IR quanta are absorbed, the molecules dissociate according to

$$DN_3 + nh\nu_6 \rightarrow ND(^1\Delta) + N_3 \qquad (n \geqq 18). \qquad (10)$$

The lowest dissociation channel involving the ground state product $ND(^3\Sigma)$ is forbidden by spin conservation.

IR irradiation of DN_3 induces a visible chemiluminescence signal. The transient behavior of the chemiluminescence signal is determined by the following secondary reactions[27]:

$$ND(^1\Delta) + DN_3 \xrightarrow{k_1} ND_2(^2A_1) + N_3, \qquad (11)$$

$$ND(^1\Delta) + DN_3 \xrightarrow{k_2} ND_2(^2B_1) + N_3, \qquad (12)$$

$$ND_2(^2A_1) \xrightarrow{k_{rad}} ND_2(^2B_1) + h\nu_{visible}, \qquad (13)$$

$$ND_2(^2A_1) + DN_3 \xrightarrow{k_3} ND_2(^2B_1) + DN_3, \qquad (14)$$

$$ND_2(^2A_1) + DN_3 \xrightarrow{k_4} ND_3 + N_3. \qquad (15)$$

The IRMPE of DN_3 has been studied[29] and is summarized below.

(a) The chemiluminescence signals induced by 0.5 ns CO_2 pulses have been measured as a function of the pressure. The following analysis has been performed to confirm that the dissociation of DN_3 is indeed collision free. In a collisionless dissociation process the number n_{ND} of $ND(^1\Delta)$ products is given by

$$n_{ND} = N_0 Y_{diss}(\Phi), \qquad (16)$$

where N_0 is the number of DN_3 molecules in the collimated excitation zone and $Y_{diss}(\Phi)$ is the fluence-dependent dissociation yield. The ND excited intermediate is further scavenged to produce excited ND_2^* species and the number of ND_2^* molecules produced is

$$n_{ND_2^*} = \frac{k_1}{k_1 + k_2} N_0 Y_{diss}(\Phi) \equiv Y'(\Phi)p,$$

where p is the pressure of the DN_3 sample. The fluorescence yield Y_F depends on the DN_3 pressure. One has

$$Y_F = \frac{k_{rad}}{k_{rad} + (k_3 + k_4)p}, \qquad (17)$$

while the number of photons emitted following CO_2 laser excitation is given by

$$S = n_{ND_2^*} Y_F. \qquad (18)$$

Thus

$$S^{-1} = \left[\frac{k_3 + k_4}{k_{rad}} + p^{-1}\right] Y'^{-1}(\Phi). \qquad (19)$$

For 0.5 ns pulses the pressure dependence of the observed fluorescence is found to be consistent with Eq. (19).

(b) The induced chemiluminescence signals have been calibrated to absolute dissociation yields. This has been achieved by comparing the IR induced signals with the chemiluminescence resulting from UV dissociation of DN_3 by 266 nm quadrupled Nd:Yg pulses. The yields, as a function of the CO_2 laser fluence, are shown in Fig. 9 for excitations by 0.5 ns and 30 ns CO_2 pulses. The intensity dependence, or pulse duration dependence, is quite pronounced, although not as strong as for SO_2.

(c) Optoacoustic measurements have also been performed. The results are shown in Fig. 10. Once again the crucial dependence on the intensity of the IR pulse is demonstrated. Comparing the average number of photons absorbed with the dissociation yields, one observes that $\langle n \rangle \gg 18\ Y_{diss}$ photons for the whole fluence range. In contrast with the case of SO_2, IR absorption by DN_3 does result in the population of intermediate discrete vibrational levels.

(d) When the chemiluminescence spectrum of ND_2 is compared with the reported spectrum induced by UV dissociation of HN_3,[27] the IR induced spectrum is found to be blue-shifted by 1 eV. Analysis of the UV dissociative process[27] shows that only vibrationless $NH(^1\Delta)$ species are produced in the UV dissociation process. The short wavelength cut at 600 nm of the UV induced

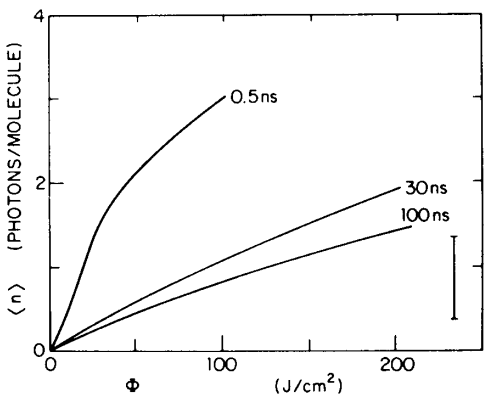

Fig. 9. Average number of photons absorbed per DN_3 molecules as a function of energy fluence for CO_2 laser pulses of different duration.

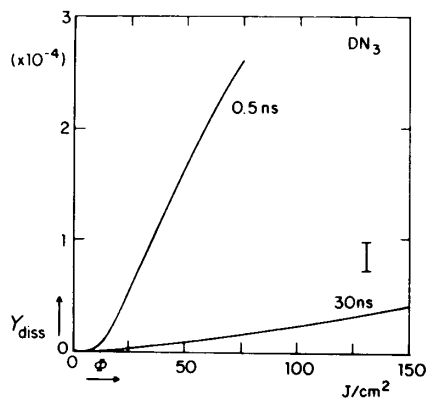

Fig. 10. Dissociation yield of DN_3 as a function of energy fluence for CO_2 pulses of different duration.

chemiluminescence is consistent with the exothermicity of the reaction

$$NH(^1\Delta) + HN_3 \rightarrow NH_2(^2B_1) + N_3.$$

On the other hand, the 8,000 cm^{-1} shift observed for the IRMPD process is attributed to the formation of vibrationally excited $ND(^1\Delta)$. Since DN_3 has six vibrational degrees of freedom, only a fraction of the excess energy above the dissociation limit is expected to go into ND vibrations. The presence of ND with 1 eV or more vibrational excitation implies excitation of DN_3 far above the dissociation limit. Furthermore, the spectral distribution is independent of the fluence of the CO_2 pulses and of the pulse duration. This observation is hard to explain on the basis of a competition between the up-pumping rate and RRKM dissociation rate. Since the up-pumping rate changes with intensity, one expects the ratio of the shifted blue to red fluorescence to be intensity-dependent.

An alternative speculation is that the RRKM model, involving statistical distribution of the vibrational energy, is not obeyed for hydrazoic acid. This is also indicated by recent measurements[28] of the overtone spectra of HN_3, which show that up to the dissociation limit very little mixing of the overtone with the dense manifold occurs.

VII. CONCLUSION

These data on small molecules, with *verified collisionless* excitation, show that there exists a gradual transition from the regime of discrete states to the quasicontinuum regime. In diatomic molecules one has a pure discrete case. The power threshold required for dissociation is so high that ionization would take place before dissociation. Very large molecules with heavy atoms at or above room temperature are always in the quasicontinuum regime and exhibit a strict fluence dependence of excitation. Black[30] has shown that intensity dependent effects become gradually more pronounced as the size and weight of the molecules becomes smaller. The excitation of triatomic molecules is predominantly determined by the intensity. Most molecules in the initial rotational manifold remain unexcited. A small fraction may be excited in a multiphoton process. The density of states in the quasicontinuum is enhanced over that calculated from the Whitten–Rabinowitch formula, because of a breakdown of rotational selection rules in the highy excited manifold. Once excited to such high levels, dissociation of the small molecule can readily follow. The gradual transition in the IRMPE behavior from diatomic molecules to large polyatomic molecules is indicated in Table 1. This table relates the present data to the extensive earlier IRMPE work on large molecules. A gradual transition occurs with the change in the degree of vibrational excitation at which the inequalities mentioned in the introduction become satisfied. This defines the diffuse boundary between the discrete level regime (region one) and the quasicontinuum. For small molecules the crossing of region one by an intensity-dependent multiphoton process constitutes the rate-determining step for IRMPE and IRMPD.

This work summarizes the results contained in the Ph.D. thesis by one of us.[7] It was supported by the U.S. Army Research Office under contract no. DAAG29-81-K-0071.

REFERENCES

1. N. R. Isenor, V. Merchant, R. S. Hallsworth and M. C. Richardson, *Can. J. Phys.*, **51**, 1281 (1973).
2. For a recent review see: W. Fuss and K. L. Kompa, *Prog. Quantum Electron.*, **7**, 117 (1981).
3. a. N. Bloembergen and E. Yablonovitch, *Phys. Today*, **31**, 23 (1978). b. V. S. Letokhov, *Nonlinear Laser Chemistry*, Chemical Physics Vol. 22, Springer, Heidelberg, 1983.
4. J. G. Black, P. Kolodner, M. J. Shultz, E. Yablonovitch and N. Bloembergen, *Phys. Rev. A*, **19**, 704 (1979).
5. I. Scheck and J. Jortner, *J. Chem. Phys.*, **70**, 3016 (1979).
6. B. Carmeli and A. Nitzan, *J. Chem. Phys.*, **72**, 2070 (1980).
7. T. B. Simpson, Ph.D. thesis, Harvard University, 1983 (unpublished).
8. J. R. Stine and D. W. Noid, *Opt. Cammun.*, **31**, 161 (1979).
9. G. L. Peterson, C. D. Cantrell and R. S. Burkey, *Opt. Commun.*, **43**, 123 (1982).
10. G. L. Wolk, R. E. Weston and G. W. Flynn, *J. Chem. Phys.*, **73**, 1649 (1980).
11. D. Proch and H. Schröder, *Chem. Phys. Lett.*, **61**, 426 (1979).
12. Ph. Avouris, M. M. T. Loy and I. Y. Chan, *Chem. Phys. Lett.*, **63**, 624 (1979).
13. A. Hartford, *Chem. Phys. Lett.*, **57**, 352 (1978).
14. J. Y. Tsao, T. B. Simpson, N. Bloembergen and I. Burak, *J. Chem. Phys.*, **77**, 1274 (1982).

Table 1. Trends in IR Multiphoton Excitation

Diatomics	3 and 4 atom molecules	4–6 atom molecules	6–10 atom molecules	10+ atom molecules
Strict multiphoton excitation	Intensity controls excitation	Both intensity, fluence important	Fluence dominates intensity	Fluence controls excitation
No known examples of IR dissociation	At 100 GW/cm^2: -small diss. yield -small $\langle n \rangle$	Unity dissociation yield, 10–50 J/cm^2 lower for < 1 ns t_p	Unity dissociation yield, 10 J/cm^2	Unity dissociation yield, 1–10 J/cm^2
Theoretical calc. estimates		Large bottleneck	Small bottleneck	No bottleneck
10–100 TW/cm^2 for dissociation	Region one dominates	Both region one, quasicon. effects	Quasicontinuum dominates	Molecule starts in quasicontinuum

Region One	*Quasicontinuum*
Excitation via resonantly enhanced high order multiphoton processes to quasicontinuum	One-photon, stepwise, incoherent excitation
Little population of intermediate excited states due to lack of resonances	Broad distribution of final excited states

15. T. B. Simpson and N. Bloembergen, *Opt. Commun.*, **37**, 256 (1981).
16. C. J. Halstead and B. A. Thrush, *Proc. R. Soc. London, Ser. A*, **295**, 363 (1966).
17. T. B. Simpson and N. Bloembergen, *Chem. Phys. Lett.*, to appear.
18. M. Bixon and J. Jortner, *J. Chem. Phys.*, **50**, 3284 (1969).
19. H. D. Mettee, *J. Chem. Phys.*, **49**, 1784 (1968).
20. L. E. Brus and J. R. McDonald, *J. Chem. Phys.*, **61**, 97 (1974).
21. F. Su, J. W. Bottenheim, H. W. Sidebottom, J. G. Calvert and E. K. Damon, *Int. J. Chem. Kinet.*, **10**, 125 (1978).
22. V. M. Donnelly, D. G. Keil and F. Kaufman, *J. Chem. Phys.*, **71**, 659 (1979).
23. S. Kimel, D. Feldman, J. Laukemper and K. H. Welge, *J. Chem. Phys.*, **76**, 4893 (1982).
24. I. Burak, J. Y. Tsao, Y. Prior and E. Yablonovitch, *Chem. Phys. Lett.*, **68**, 31 (1979).
25. W. M. Uselman and E. K. C. Lee, *J. Chem. Phys.*, **64**, 3475 (1976).
26. K. H. Welge and H. Zacharias, private communication.
27. A. P. Baronavski, R. G. Miller and J. R. McDonald, *Chem. Phys.*, **30**, 119 (1978).
28. K. K. Lehmann, G. J. Scherer and W. Klemperer, to appear.
29. T. B. Simpson, E. Mazur, K. K. Lehmann, I. Burak and N. Bloembergen, *J. Chem. Phys.*, **79**, 3373 (1983).
30. J. G. Black, Ph.D. thesis, Harvard University, 1980 (unpublished).